Article

pubs.acs.org/Biomac

Dual Stimuli-Responsive Poly(*N*-isopropylacrylamide)-*b*-poly(L-histidine) Chimeric Materials for the Controlled Delivery of Doxorubicin into Liver Carcinoma

Renjith P. Johnson,[†] Young−Il Jeong,[‡] Johnson V. John,[†] Chung-Wook Chung,[‡] Dae Hwan Kang,[‡] Manickam Selvaraj,[§] Hongsuk Suh,[∥] and Il Kim*[,†]

[†]The WCU Center for Synthetic Polymer Bioconjugate Hybrid Materials, Department of Polymer Science and Engineering, [§]School of Chemical and Biomolecular Engineering, and [∥]Department of Chemistry and Chemistry Institute for Functional Materials, Pusan National University, Pusan 609-735, Republic of Korea

[‡]National Research and Development Center for Hepatobiliary Cancer, Pusan National University, Yangsan Hospital, Yangsan 626-870, Republic of Korea

Supporting Information

ABSTRACT: A series of dual stimuli responsive synthetic polymer bioconjugate chimeric materials, poly(*N*-isopropylacrylamide)$_{55}$-*block*-poly(L-histidine)$_n$ [p(NIPAM)$_{55}$-*b*-p(His)$_n$] (n = 50, 75, 100, 125), have been synthesized by employing reversible addition−fragmentation chain transfer polymerization of NIPAM, followed by ring−opening polymerization of α-amino acid *N*-carboxyanhydrides. The dual stimuli responsive properties of the resulting biocompatiable and membrenolytic p(NIPAM)$_{55}$-*b*-p(His)$_n$ polymers are investigated for their use as a stimuli responsive drug carrier for tumor targeting. Highly uniform self-assembled micelles (~55 nm) fabricated by p(NIPAM)$_{55}$-*b*-p(His)$_n$ polymers display sharp thermal and pH responses in aqueous media. An anticancer drug, doxorubicin (Dox), is effectively encapsulated in the micelles and the controlled Dox release is investigated in different temperature and pH conditions. Antitumor effect of the released Dox is also assessed using the HepG2 human hepatocellular carcinoma cell lines. Dox molecules released from the [p(NIPAM)$_{55}$-*b*-p(His)$_n$] micelles remain biologically active and have stimuli responsive capability to kill cancer cells. The self-assembling ability of these hybrid materials into uniform micelles and their efficiency to encapsulate Dox makes them a promising drug carrier to cancer cells. The new chimeric materials thus display tunable properties that can make them useful for a molecular switching device and controlled drug delivery applications needing responses to temperature and pH for the improvement of cancer chemotherapy.

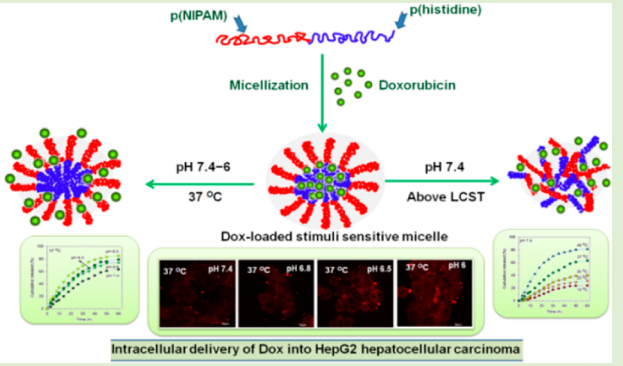

1. INTRODUCTION

Water-soluble polymers that undergo phase transition in response to environmental stimuli are widely used in various biomedical applications.[1] The ability to reversibly trigger and control the properties of these systems via the application of external stimuli offers a great promise in designing drug and gene delivery systems.[2] Especially, peptide copolymers provide many advantages over conventional synthetic polymers due to their ability to hierarchically assemble into stable ordered conformations.[3] Bioconjugates with dual stimuli-responsive polymers are particularly interesting because their responsive nature can be conferred to the attached biological component.[4] They can also show interesting properties such as thermoreversible aggregation and gelation and have been found use as promising biomaterials for variety of applications.[5] In the recent years, much effort has been focused on the synthesis of water-soluble (co)polymers that undergo a conformational change, or phase transition, in response to external stimuli,[6] such as temperature, added electrolyte, and changes in pH, light, magnetic field, and ultrasound, and a combination of any of these. Among these stimuli changes, temperature and pH are ideal in terms of easy and safe for any biomedical applications.

Poly(*N*-isopropylacrylamide) [p(NIPAM)] is a key member of the temperature responsive polymers, not only in drug delivery but in biomedical and intelligent material studies concerning hydrogels and bioconjugates. The toxicity of p(NIPAM) can be a problem for in vivo use, even though copolymerization with nontoxic peptides is an effective approach to achieve a biocompatable stimuli responsive drug delivery system. It is well-known that p(NIPAM) can show coil to globule transition above the lower critical solution temperature (LCST) at 32 °C in aqueous solution.[7] The

Received: January 18, 2013
Revised: April 8, 2013

   dx.doi.org/10.1021/bm400089m | *Biomacromolecules* XXXX, XXX, XXX−XXX

LCST of p(NIPAM) can be easily tuned to a desired temperature by copolymerization with pH sensitive comonomers, yielding NIPAM copolymers in which the phase transition can be triggered by a change in the pH at specific temperature.[8,9] There are typically two kinds of p(NIPAM) containing block copolymers reported in the literature. First the double hydrophilic block copolymers, in which p(NIPAM) coupled to a hydrophilic block, soluble in aqueous media at low temperatures and form micelles p(NIPAM) cores above the LCST of p(NIPAM).[10−14] The other class of amphiphilic copolymers in which p(NIPAM) coupled to a hydrophobic block such as polystyrene, polylactide, and poly(L-lysine).[15−18] These block copolymers self-assemble with hydrophobic cores and hydrophilic p(NIPAM) coronas below its LCST. Recently developed controlled living radical polymerizations (CLRP)[19−21] afford (co)polymers with controlled molecular weight (MW), low polydispersity (PD), and well-defined architectures. Among CLRPs, reversible addition−fragmentation chain transfer (RAFT) is versatile in that the leaving and the activating groups of the thiocarbonylthio compound are retained at the ends of the resulting polymers, affording the preparation of polymers with specific functional end groups by the choice of appropriate RAFT agents or by post-functionalizations.[22]

The synthetic polymers conjugated with polypeptides lead to a promising class of block copolymers widely termed as "macromolecular chimera."[23,24] Only few research activities have been focused on dual stimuli-responsive block copolymers consisting of pH sensitive polypeptides and thermosensitive synthetic polymer segments.[18,25−27] The most common copolypeptides in this category are based on glutamic acid and lysine.[27] Recently, Giani et al. investigated a thermo- and pH-sensitive aggregation behavior of dual responsive poly(*N*,*N*-diethylacrylamide)-*b*-poly-(L-lysine) in aqueous solution.[28] The critical transitions of pH responsive copolymers of p(NIPAM) with acrylic monomers are usually below pH 5 due to their low pK_b values. In this juncture, we found poly(L-histidine) [p(His)] is an excellent candidate and it is different from other amino acids due to the sharp pH sensitivity, nontoxic nature, biocompatibility, nutritional functions, and the enhanced pharmacological efficiency. The physiologically relevant pH range is from 5.0 to 7.4, if the protonation of polymers only occurs within this pH range, they are suitable for fabricating the pH-responsive materials for biomedical applications. Most importantly, the fusogenic activity of p(His) can disrupt the enveloped membrane of acidic subcellular compartments such as endosomes, thus, resulting in drug/nucleic acids reaching the cytosol[29] to enhance the delivery efficiency. Thus, the polymeric micelle system with a p(His) core or corona could be an effective mode for the controlled drug release.

Recently, Carlsen and Lecommandoux reviewed the self-assembly of various polypeptide based block copolymer amphiphiles[30] and polypeptide based systems for Dox delivery.[31,32] In our previous contribution, biocompatiable doxorubicin (Dox)-loaded pH-sensitive micelles demonstrated successfully controlled release and in vitro cytotoxicity against HCT-116 human colon carcinoma cells.[33] Here, we focus on a new bioconjugate combining a temperature responsive p(NIPAM) as the synthetic polymer segment with a pH responsive p(His) as the polypeptide block. The p(NIPAM)-*b*-p(His) chimeras were successfully synthesized by combining RAFT with ring-opening polymerization (ROP). A newly designed RAFT chain transfer agent (CTA) was synthesized and applied for the CLRP of NIPAM and the successive ROP of benzyl-*N*-carboxy-L-histidine anhydride (Bn-His-NCA) using p(NIPAM)-NH_2 macroinitiator prepared by the end-group functionalization. The benzyl groups were finally deprotected for further investigations. Micelles were fabricated by the self-assembly of the copolymers and Dox was encapsulated for the evaluation of the drug-loading and drug-release behaviors in various pH and temperature conditions. The cytotoxicity of the micelles was tested with HepG2 and RAW264.7 (a leukemic monocyte macrophage cells) cell lines. The stimuli-responsive anticancer effect of the released Dox has been investigated using HepG2 hepatocellular carcinoma cell lines.

2. EXPERIMENTAL SECTION

2.1. Materials. 1-Dodecanethiol (98.5%), tetramethylammonium bromide (98.5%), carbon disulfide (99.9%), 2-amino ethanol (97%), paratoluene sulfonyl chloride (99%), triethylamine (TEA, 99.5%), 4-(dimethylamino)pyridine (DMAP, 99%), *N*,*N*′-dicyclohexylcarbodiimide (DCC, 99.0%), 2,2′-azobis(2-methylpropionitrile (AIBN 98%), and doxorubicin hydrochloride (Dox) were purchased from Sigma-Aldrich and used without further purification. *N*-*α*-*t*-Butyloxycarbonyl-*N*-im-benzyl-L-histidine (Boc-L-His-(Bzl)-OH) purchased from Bachem and used without further purification. *N*-Isopropylacrylamide (NIPAM, 97% Acros) was recrystallized from hexane. *N*,*N*-Dimethylformamide (DMF) and *N*,*N*-dimethyl acetamide (DMAc) was distilled over sodium. Acetone and chloroform were distilled over calcium hydride. 1,4-Dioxane was purified by column chromatography on activated Al_2O_3 to remove peroxide impurities and then distilled. All other reagent grade of chemicals were purchased from Sigma-Aldrich or TCI and used without furthur purification.

2.2. Instrumentation and Measurements. ^{1}H NMR (400 MHz) and ^{13}C NMR (100 MHz) spectra were recorded on a Varian INOVA 400 NMR spectrometer. The temperature-dependent ^{1}H NMR measurement was performed after the sample tube was kept at each preset temperature around 10 min for equilibrium. Chemical shifts are reported in parts per million (ppm) relative to the residual solvent peaks as internal standard. Peak multiplicities in ^{1}H NMR spectra are abbreviated as s (singlet), d (doublet), t (triplet), m (multiplet), and br (broad). Column chromatography was performed using a Combi-Flash Companion purification systems (Teledyne ISCO) using silica gel of 300−400 mesh. UV−vis turbidimetry experiments were carried out for LCST determination on a shimadzu UV-1650 PC, equipped with a temperature controller. Fourier-transform infrared (FT-IR) spectra were recorded on a shimadzu IR prestige 21 spectrometer at room temperature. The spectra were taken on KBr discs at the range of 3500−500 cm^{-1}. The molecular weight (MW) and polydispersity index ($Đ$) of the polymers were measured on a Waters GPC system, which was equipped with a Waters 1515 HPLC solvent pump, a Waters 2414 refractive index detector, and three Waters Styragel High Resolution columns (HR4, HR2, HR1, effective molecular weight range 5000−500000, 500−20000, and 100−5000 g mol^{-1}, respectively) at 40 °C using HPLC grade THF containing 0.1 N LiBr as eluent at a flow rate of 1.0 mL/min. Monodispersed polystyrenes were used to generate the calibration curve.

DLS measurements were performed with a high performance Zetasizer Nano ZS90 (Malvern Instruments, Ltd., U.K.) with a He−Ne laser (633 nm) and 90° collecting optics and a thermoelectric pelteir temperature controller. Block copolymer solutions (2 mg·mL^{-1}) were filtered through a 0.5 μm filter prior to use. Temperature-dependent DLS experiments were performed after the equilibration of the samples for 10 min. Transmission electron microscopy (TEM) was performed on a JEOL−1299EX TEM with an accelerating voltage of 80 keV. TEM grids were treated with oxygen plasma (from a Harrick plasma cleaner/sterilizer) for 20 s to render their surface hydrophilic. $(NH_4)_2MoO_4$ (2 mL; 2% aqueous solution by weight), water (5 mL), and polymer micelles (3 mL) were mixed

on the surface of a plastic Petri dish to form a small bead. A TEM grid was then floated on top of the bead with the hydrophilic face contacting the solution. The TEM grid was carefully removed with a pair of tweezers, wicked with a filter paper to remove excess liquid, and then dried in air for 1 min.

2.3. Synthesis of Tosyl-Protected 2-Amino Ethanol. 2-Amino ethanol (1.50 mL, 25 mmol) and triethylamine (TEA, 7 mL, 50 mmol) dissolved in anhydrous THF (20 mL) were fed to a 100 mL Schlenk flask fitted with a N_2 inlet and a rubber septum and were cooled in an ice bath. A THF solution of *para*-toluene sulfonyl chloride (4.76 g, 25 mmol) was added to the mixture dropwise. White precipitate of triethylammonium salt was observed and the reaction was allowed to stir at room temperature overnight. After the precipitate was filtered off, THF was removed by rotary evaporation. The residue was purified with flash column (silica gel, hexane/ethyl acetate, *v*/*v* 4/2), affording the product as a white solid. Yield: 61%. ^{1}H NMR (400 MHz, $CDCl_3$ δ): 2.10 (t, 1H, OH), 4.30 (t, 1H, NH), 2.35 (s, 3H, CH_3), 3.36 (m, 2H, $NHCH_2$), 3.82 (m, 2H, $HOCH_2$), 7.34 (m, 2H, H_{meta}), 7.82 (m, 2H, H_{ortho}) ppm. ^{13}C NMR (100 MHz, $CDCl_3$ δ): 20.8, 43.2, 63.4, 125.8, 129.6, 136.3, 141.4 ppm.

2.4. Synthesis of Tosyl-Protected RAFT Chain Transfer Agent (CTA-2). A dry dichloromethane (10 mL) solution of CTA 1 (0.364 g, 1 mmol) and tosyl-protected 2-amino ethanol (0.215 g, 1 mmol) was cooled in an ice bath. 4-(*N*,*N*′-Dimethylamino)pyridine (DMAP, 0.025 g, 0.2 mmol) and 1,3-dicyclohexylcarbodiimide (DCC, 0.26 g, 1.25 mmol) were added in 30 min, and the mixture was stirred at room temperature for 24 h. The resultant reaction mixture was filtered, concentrated, and the residue was purified by flash column (silica gel, petroleum ether/ethyl acetate, *v*/*v* 5/1), affording the product as a pale yellow solid. Yield: 41%. ^{1}H NMR (400 MHz, $CDCl_3$ δ): 0.98 (t, 3H, $CH_3C_{10}H_{20}CH_2$-), 1.64 (m, 6H, $SC(CH_3)_2$-, 1.30−1.96 (m, 20H, $CH_3C_{10}H_{20}CH_2$-), 2.35 (s, 3H, CH_3), 2.90 (t, 2H SCH_2), 3.50 (m, 2H, $NHCH_2$), 4.30 (t, 1H, NH), 4.40 (m, 2H, OCH_2), 7.34 (m, 2H, H_{meta}), 7.82 (m, 2H, H_{ortho}) ppm. ^{13}C NMR (100 MHz, $CDCl_3$ δ): 14.8, 20.9, 22.8, 23.1, 28.9, 30.2, 30.4, 31.1, 32.5 34.3, 40.8, 52.8, 67.5, 125.4, 129.3, 136.4, 140. 2, 174.5, 208.7 ppm.

2.5. Polymerization of NIPAM from CTA-2. A Schlenk tube containing reaction solution (4 mL) of NIPAM (1.1760 g, 10.4 mmol), CTA-2 (66.1 mg, 0.1 mmol), and AIBN (3.344 mg, 0.02 mmol) in DMF was degassed by freeze−pump−thaw cycles for three times and the solution was stirred at 70 °C under N_2 for 24 h. Precipitation in ethyl ether twice afforded ω-tosylated p(NIPAM) [p(NIPAM)-Ts] as a white powder ($M_{n,GPC}$ = 13800). ^{1}H NMR (400 MHz, $CDCl_3$ δ): 0.98 (t, 3H, $CH_3C_{10}H_{20}CH_2$-), 1.28 (br, $CH(CH_3)_2$, 1.30−1.96 (br, 20H, $CH_3C_{10}H_{20}CH_2$-), 2.52 (br, CH_2), 3.47 (br, CH), 3.94 (br, CH), 4.30 (t, 1H, NH), 4.40 (m, 2H, OCH_2), 6.21 (br, NH) 7.34 (m, 2H, H_{meta}), 7.82 (m, 2H, H_{ortho}) ppm. ^{13}C NMR (100 MHz, $CDCl_3$ δ): 14.08, 20.9, 21.6 23.1, 23.81, 23.1, 28.9, 30.3, 30.9, 31.7, 32.5, 34.1, 39.4, 40.3,41.3, 45.6, 52.8, 67.5, 125.4, 129. 3, 136.4, 140.2, 174.1, 174.5, 208.7 ppm.

2.6. Synthesis of p(NIPAM)-NH_2·HBr. p(NIPAM)-Ts (0.91 g, 0.130 mmol) was dissolved in methanol (4 mL) at 0 °C. HBr in acetic acid (2 mL) was then added dropwise. After stirring for 2 h, an excess amount of methanol was added. The polymer was precipitated in diethyl ether twice and dried under vacuum at 40 °C for 24 h, yielding the targeting polymer as a pale yellow powder ($M_{n,GPC}$ = 14700). ^{1}H NMR (400 MHz, $CDCl_3$ δ): 0.98 (t, 3H, $CH_3C_{10}H_{20}CH_2$-), 1.25−1.96 (br, 20H, $CH(CH_3)_2$, 2.52 (br,CH_2) 2.90 (t, 2H SCH_2), 3.47 (br, CH), 3.94 (br, CH), 4.30 (t, 1H, NH), 4.40 (m, 2H, OCH_2), 6.21 (br, NH) ppm. ^{13}C NMR (100 MHz, $CDCl_3$ δ): 14.08, 20.9, 21.6, 23.7, 23.8, 23.1, 28.9, 30.1, 30.3, 31.1, 32.5, 34.3, 39.4, 40.3, 41.3, 45.6, 174.1, 174.5, 208.7 ppm.

2.7. Synthesis of p(NIPAM)-NH_2. KOH in MeOH solution (1 mol/L) was dropped at room temperature to the solution of p(NIPAM)-NH_2·HBr (0.80 g, 0.112 mmol) in MeOH (4 mL) to adjust the pH to 11. After stirring for 1 h, the polymer was precipitated in diethyl ether twice, yielding the polymer as a white powder (0.71 g, 90%, $M_{n,GPC}$ = 13300). ^{1}H NMR (400 MHz, $CDCl_3$ δ): 0.94 (t, 3H, $CH_3C_{10}H_{20}CH_2$-), 1.25−1.96 (br, 20H, $CH(CH_3)_2$, 2.52 (br,CH_2), 2.90 (t, 2H SCH_2), 3.47 (br, CH), 3.94 (br, CH), 4.30 (t, 1H, NH), 4.40 (m, 2H, OCH_2), 6.21 (br, NH) ppm. ^{13}C NMR (100 MHz, $CDCl_3$ δ): 14.08, 20.9, 21.6, 23.7, 23.8, 23.1, 28.9, 30.1, 30.3, 31.1, 32.5, 34.3, 39.4, 40.3, 41.3, 45.6, 174.1, 174.5, 208.7 ppm.

2.8. Synthesis of p(NIPAM)-*b*-p(His). Bn-His-NCA was previously synthesized for the ROP initiated by p(NIPAM)$_{55}$-NH_2. Boc-L-His-(Bn)-OH (2.5 g) was suspended in anhydrous 1,4-dioxane (10 mL) to which a solution of PCl_5 (1.8 g) in 1,4-dioxane (20 mL) was added to form the Bn-His-NCA at 25 °C under stirring. Within a few minutes, a clear solution was obtained, which was then filtered through a glass filter. Crystals of Bn-His-NCA were obtained after the addition of the filtrate to an excess of diethyl ether. The product was subsequently washed and dried under vacuum. For the ROP of Bn-His-NCA by using p(NIPAM)-NH_2 as a macroinitiator, the p(NIPAM)-NH_2 (0.61 g, 0.10 mmol) and predetermined amount of Bn-His-NCA were dissolved in DMF in two separate Schlenk flasks and subsequently combined using a transfer needle under nitrogen. The reaction mixture was stirred for 72 h at room temperature under a nitrogen atmosphere. After polymerization, the solvent was concentrated under high vacuum. The concentrated DMF solution was precipitated in anhydrous diethyl ether and dried under vacuum to yield p(NIPAM)$_{55}$-*b*-p(Bn−His)$_n$ (n = 50, 75, 100, 125).

For the deprotection of the benzyl groups, a round-bottomed flask was charged with a solution of the p(NIPAM)$_{55}$-*b*-p(Bn-His)$_n$ in trifluoroacetic acid (100 mg, 3 mL). Then, a 4-fold molar excess of a 33 wt % solution of HBr in acetic acid was added, and the reaction mixture was stirred for 2 h at 0 °C. Finally, the reaction mixture was precipitated in anhydrous diethyl ether. Polymer is isolated and subjected to aminolysis in presence of hexylamine and few drops of $Na_2S_2O_4$ in DMF, and then the reaction mixture was precipitated in ether. Finally, the product was furthur purified by dialysis and subsequently freeze-dried to yield p(NIPAM)$_{55}$-*b*-p(His)$_n$ (n = 50, 75, 100, 125). ^{1}H NMR (400 MHz, $CDCl_3$ δ): 1.25−1.43 (br, $CH(CH_3)_2$, 2.51 (br, CH_2), 3.01 (d, nH, CH_2), 3.47 (br, $CH(CH_2)$, 3.95 (t, nH, CH), 6.87 (br, Ar-H), 6.97 (br, Ar-H), 8.10 (br, NH), 9.35 (br, Ar-NH) ppm. ^{13}C NMR (100 MHz, $CDCl_3$ δ): 21.6, 23.7, 34.5, 36.2, 39.5, 41.6 45.3, 60.7, 122.3, 148.5, 175.4 ppm.

2.9. Fabrication of Micelles. Micelles were prepared by combining a self-assembly derived precipitation with a membrane dialysis method. p(NIPAM)$_{55}$-*b*-p(His)$_n$ (10 mg) was dissolved in DMAc and then deionized water (3 mL) was added into the polymer solution. The turbid mixture was then dialyzed aginist deionized water for 2 d using a dialysis membrane (regenerated cellulose) with a molecular weight cut-off 2000 (MWCO = 2000) at 25 °C. The outer phase was replaced at 3 h intervals with fresh water. The solution was subsequently lyophilized after filtering through a 0.2 μm syringe filter in order to remove any impurities and non−micellar aggregates (yield = 63%).

For Dox-loaded micelles, Dox (20 mg) dissolved in DMAc (7 mL) and TEA (1.5 equivalent to Dox) was added to the solution of block copolymer (20 mg) dissolved in DMAc (7 mL) at room temperature with mixing. After adding 6 mL of water into the solution, the resulting drug-loaded micelle solution was then dialyzed against deionized water using a dialysis membrane (MWCO = 2000) at 25 °C for 2 d (yield = 58%).

2.10. Determination of Drug-Loading Content (DLC), Efficiency (DLE), and In Vitro Drug Release. For the quantification of the amount of drug encapsulated, aliquots of the drug-loaded micelle solution were lyophilized and broken up by adding 2 mL of DMSO. The obtained solution was analyzed using the UV−vis spectroscopy. The characteristic absorbance of Dox (485 nm) was recorded and compared with a standard curve generated in DMF of drug concentrations varying from 0−100 mg/mL. The percentages of DLC and DLE were calculated according to the following equations.

$$\mathrm{DLC}(\%) = (\text{weight of drug in the micelle} / \text{weight of drug-loaded micelle}) \times 100$$

dx.doi.org/10.1021/bm400089m | *Biomacromolecules* XXXX, XXX, XXX−XXX

Scheme 1. Synthesis of p(NIPAM)-*b*-p(His) and the Fabrication of the Dual Stimuli Responsive Drug-Loaded Micelles for the Controlled Delivery of Doxorubicin

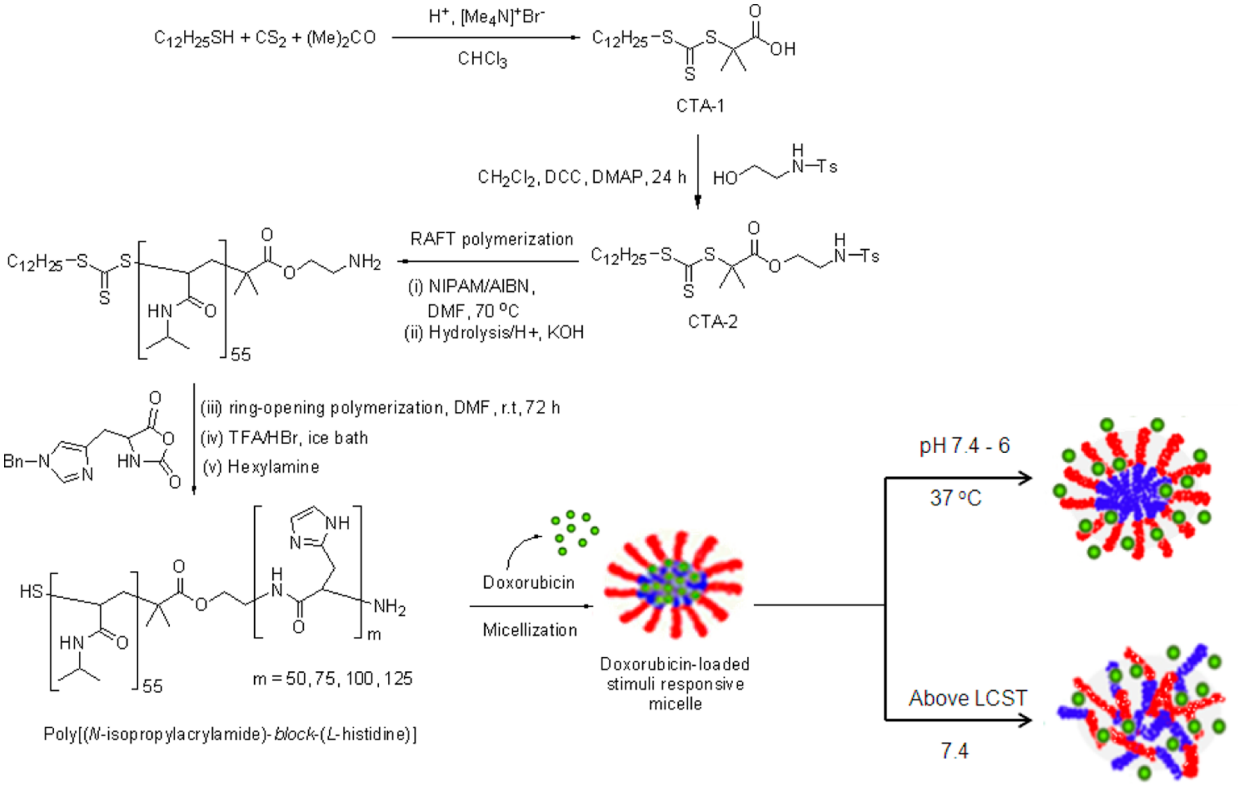

$$\text{DLE}(\%) = (\text{weight of drug in the micelle}/\text{weight of drug for drug-loaded micelle preparation}) \times 100$$

For in vitro drug release studies, a prescribed amount of Dox-loaded micelle solution suspended in dialysis bags was placed into buffer solution [phosphate-buffered saline (PBS), 20 mL] with the required pH value. Then, the samples were placed in a shaking bath at 70 rpm and at the required temperature. The buffer solution was periodically replaced with a fresh solution and the amount of released drug was measured by UV–vis spectroscopy. The drug concentration was determined according to the standard curves for the drug solution at different pH values.

2.11. Cell Culture and Confocal Laser Scanning Microscopy (CLSM). HepG2 hepatocellular carcinoma cells were cultured in DMEM medium supplemented with 10% fetal bovine serum, at 37 °C and 5% CO_2 atmosphere. HepG2 cells were seeded in 6-well plates with 1000 μL of medium and then incubated overnight in a CO_2 incubator (5% CO_2) at 37 °C. A total of 24 h later, Dox-loaded micelles were added to the cells and incubated for 1 h. Cells were then washed with PBS (pH 7.4, 0.1 M) and treated with 4% paraformaldehyde and fixed by immobilization solution (IMMU–MOUNT, Thermo Electron Corporation). These cells were observed with a CLSM (Leica TCS-SP2).

2.12. Cytotoxicity Studies and Flow Cytometer Analysis. Mouse macrophage RAW264.7 and HepG2 cell lines were used to confirm cytotoxicity of the nanosized micelles of p(NIPAM)-*b*-p(His). Cells were maintained in DMEM medium supplemented with 10% fetal bovine serum (5% CO_2 at 37 °C). The viability of RAW264.7 and HepG2 cells was evaluated by thiazolyl blue tetrazolium bromide (MTT) cell proliferation assay. Cells (2×10^4) seeded in 96-well plates with 100 μL of medium were incubated overnight in a CO_2 incubator (5% CO_2 at 37 °C) and then medium was exchanged with 100 μL of serum-free medium. For cytotoxicity test, $p(NIPAM)_{55}$-*b*-$p(His)_{125}$ micelles were distributed in serum-free DMEM media and diluted to appropriate concentrations. After 2 days of incubation, 30 μL of MTT (5 mg/mL) was added to 96-well plates and incubated for 4 h. The formazan crystals formed were solubilized in DMSO, and the absorbance (560 nm, test/630 nm, reference) was determined using an automated computer-linked microplate reader (Molecular Device Co. U.S.A.). The results were expressed as a percentage of absorbance compared to that in the control cells. Each measurement was obtained as the mean value of eight wells.

The cytotoxicity of Dox-loaded micelles was measured against HepG2 hepatocellular carcinoma cells by MTT cell proliferation assay. The cells were seeded in 24-well plates at the density of 3×10^4 cells/wells and incubated in 500 μL of medium at 37 °C in 5% CO_2 for 24 h. Then the medium was removed and replaced with (500 μL) Dox-loaded micelles containing medium. Controls were treated with 0.5% *v*/*v* of DMSO. After a 4 h incubation, medium was removed and then replaced with fresh medium. After that, cells were cultured for 24 h and then 100 μL of MTT (5 mg/mL in PBS) was added to 24-well plates, followed by incubation for 4 h. The formazan crystals formed were solubilized with 100 μL DMSO, and the absorbance (560 nm, test/630 nm, reference) was determined using an automated computer-linked microplate reader and the relative cell viability was calculated. For flow cytometer analysis, Dox or Dox-loaded micelles treated HepG2 hepatocellular carcinoma cells were seeded at a density of 1×10^6 cells in six-well plates and incubated overnight. Dox-loaded micelles (10 μg Dox/mL) were added and incubated for 3 h. Cells were harvested and analyzed with a flow cytometer (Becton Dickinson FACScan). An excitation wavelength at 488 nm and emission wavelength at 522 nm were used to observe the Dox fluorescence intensity.

3. RESULTS AND DISCUSSION

3.1. Synthesis of the Amino-Functionalized RAFT Agent. The general synthetic procedures are summarized in Scheme 1. The key to successful RAFT polymerizations is the use of an appropriate CTA, which is typically a dithioesters or a trithiocarbonate. Trithiocarbonate is versatile for the design of di- or triblock copolymers directly or after the proper end

dx.doi.org/10.1021/bm400089m | *Biomacromolecules* XXXX, XXX, XXX–XXX

Table 1. Ring-Opening Polymerization Results of Bn-His-NCA Initiated by p(NIPAM)$_{55}$-NH$_2$ Macroinitiator for the Synthesis of p(NIPAM)$_{55}$-*b*-p(His)$_n$[a]

theoretical composition	B_n-His-NCA (mmol)	yield (%)	M_n[b] (g/mol) theor.[c]	NMR	GPC[d]	NMR composition	PDI[d]	LCST (°C)
p(NIPAM)$_{55}$-*b*-p(His)$_{50}$	5.0	62	13900	12800	24000	p(NIPAM)$_{55}$-*b*-p(His)$_{43}$	1.22	34.2
p(NIPAM)$_{55}$-*b*- p(His)$_{75}$	7.50	68	17350	16500	35000	p(NIPAM)$_{55}$-*b*-p(His)$_{68}$	1.28	35.7
p(NIPAM)$_{55}$-*b*-p(His)$_{100}$	10.0	70	21600	19800	44000	p(NIPAM)$_{55}$-*b*-p(His)$_{92}$	1.31	36.3
p(NIPAM)$_{55}$-*b*-p(His)$_{125}$	12.5	63	25450	23200	52000	p(NIPAM)$_{55}$-*b*-p(His)$_{114}$	1.34	37.2

[a]Conditions: p(NIPAM)$_{55}$-NH$_2$ = 0.61 g (0.10 mmol), DMF = 10 mL, temperature = 27 °C, and time = 72 h. [b]Number average molecular weight measured after deprotecting benzyl groups. [c]M_n (theoretical) = {([Bn-His-NCA]$_0$/[p(NIPAM)$_{55}$-NH$_2$]$_0$) × (MW of repeating unit after deprotecting benzyl group) + (MW of initiator)}. [d]Polydispersity index measured by GPC; DMF as eluent at 40 °C.

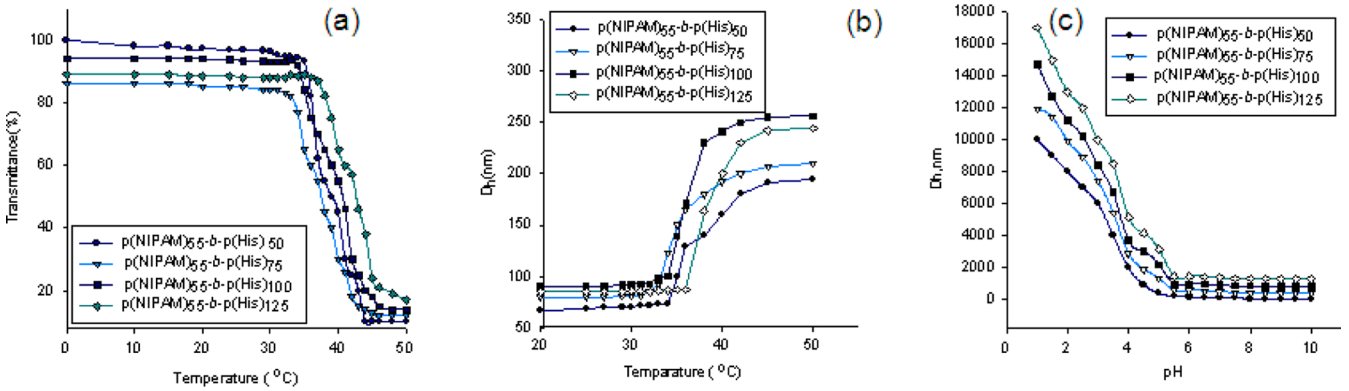

Figure 1. (a) Transmittance vs temperature curves for aqueous solution of p(NIPAM)$_{55}$-*b*-p(His)$_n$ at pH 7.4, (b) hydrodynamic diameter (D_h) vs temperature curves obtained by DLS for aqueous solutions at pH 7.4, and (c) D_h vs solution pH curves obtained by DLS for a solutions of p(NIPAM)$_{55}$-*b*-p(His)$_n$. Polymer concentration was 2.0 mg·mL^{-1} in all the experiments.

group functionalization. Recently, Boyer et al. reviewed the synthesis and bioapplications of novel hybrid materials synthesized via RAFT polymerization.[22,34] Apart from conventional amine terminated macroinitiators, Giani et al. reported the synthesis of thiol terminated poly(*N*,*N*-diethylacrylamide) via RAFT polymerization, and the resulting macro-thiol product was used for the ROP of α-(amino acid)-*N*-carboxyanhydride.[35] In this study, a new RAFT chain transfer agent with an amino functional group in the leaving group was designed (CTA-2) providing an easy way to combine the RAFT polymerization of NIPAM with the ROP of His-NCA to yield a series of p(NIPAM)$_{55}$-*b*-p(His)$_n$ (n = 50, 75, 100, 125). Amine groups in 2-aminoethanol were first protected by tosyl chloride (TsCl) and then coupled with CTA-1 via Steglich esterification reaction to afford CTA-2 as a yellow solid in 65% yield.

3.2. Synthesis of p(NIPAM)$_{55}$-*b*-p(His)$_n$ (n = 50, 75, 100, 125). The RAFT polymerization of NIPAM was performed by using CTA-2 in dimethylformamide (DMF),[27] producing p(NIPAM) with tosyl-protected amine group at the chain end (p(NIPAM)-CTA). Gel permeation chromatography (GPC) using tetrahydrofuran (THF) overestimated the MW of p(NIPAM)-CTA most probably due to the formation of intermolecular hydrogen-bonding.[36] The $Đ$ of the polymer was around 1.3. The number average MW (M_n) value of p(NIPAM)-CTA estimated by end-group analysis using nuclear magnetic resonence (NMR) spectroscopy was M_n = 7000, corresponding to about 55 repeating units of NIPAM in line with theoretical values. The p(NIPAM)$_{55}$-CTA polymer was deprotected by the acid hydrolysis to afford p(NIPAM)$_{55}$-NH$_2$. Because the purity of the p(NIPAM)$_{55}$-NH$_2$ macroinitiator is crucial in the synthesis of well-defined block copolymers with narrow $Đ$, p(NIPAM)$_{55}$-NH$_2$ was further purified by coloum chromatography with $CHCl_3$/MeOH (4:1 v/v) as eluent. After performing the ROP of Bn-His-NCA in the presence of various amounts of Bn-His-NCA by using the p(NIPAM)$_{55}$-NH$_2$ macroinitiator, p(NIPAM)$_{55}$-*b*-p(Bn-His)$_n$ (n = 50, 75, 100, 125) were precipitated in diethylether. The deprotected p(NIPAM)$_{55}$-*b*-p(His)$_n$ copolymers were finally obtained after the deprotection of the benzyl groups and the removal of the thiocarbonylthio end groups by aminolysis (Scheme 1).

All compounds synthesized were characterized by NMR spectroscopy (see Figures S1−S3 in Supporting Information, SI). The detailed polymerization results are summarized in Table 1. The $Đ$ values of the block copolymers are in the range of 1.2−1.40. The GPC elution curves and the Fourier-transform infrared (FT−IR) spectra of the block copolymers are provided in Figures S4 and S5, respectively.

3.3. Stimuli-Responsive Phase Transition Behavior of Block Copolypeptides. p(NIPAM)$_{55}$-*b*-p(His)$_n$ copolymers showed similar thermoresponsive behaviors as p(NIPAM) homopolymer. A recent study demonstrated the LCST can be varied by incorporating a hydrophilic/hydrophobic blocks in p(NIPAM).[37] The thermally induced reversible aggregation behaviors of and block copolymers have been investigated by ^{1}H NMR spectroscopy. The thermal aggregation behaviors of p(NIPAM)$_{55}$-*b*-p(His)$_n$ were investigated with ^{1}H NMR spectroscopy at a pH 7.0 with a polymer concentration of 70 mg·mL^{-1} in D_2O showed a reversible appearance and disappearance of p(NIPAM) signals when the solution temperature varied from 27 to 50 °C, demonstrating the p(NIPAM) block shows a reversible thermoresponse around its LCST due to the coil to globule transition of the p(NIPAM) chain followed by its aggregation. The temperature-dependent

dx.doi.org/10.1021/bm400089m | Biomacromolecules XXXX, XXX, XXX−XXX

^{1}H NMR spectra of p(NIPAM)$_{55}$-*b*-p(His)$_{125}$ in D_2O solution, shown in Figure S6. Signal intensities correspond to p(His) block remains unchanged in the whole temperature range with slight chemical shift changes, but those assignable to p(NIPAM) block start to decrease gradually around 31 °C and then disappeared almost completely above 42 °C.

LCST and thermal transition of p(NIPAM) block in p(NIPAM)$_{55}$-*b*-p(His)$_n$ in aqueous solution was also examined by turbidmetry measurements using UV−vis spectrometer at a polymer concentration of 2.0 mg mL^{-1} (Table 1 and Figure 1a). The block copolymers with short histidine block show LCSTs close to p(NIPAM) homopolymer; however, as the chain length of the histidine block increases, the LCST increases gradually. It was found that the LCST of p(NIPAM)$_{55}$-*b*-p(His)$_{125}$ is close to the body temperature (37.2 °C).

3.4. Dynamic Light Scattering (DLS) Measurements. The thermally induced formation of p(NIPAM) core micelles was investigated by using dynamic light scattering (DLS) technique. Figure 1b shows the temperature dependence of scattered light intensity and average hydrodynamic diameter (D_h) obtained for an aqueous solution of p(NIPAM)$_{55}$-*b*-p(His)$_n$ at pH 7.4. Below 30 °C, the block copolymers are molecularly dissolved with D_h of about 14 nm and very weak scattered light intensity. When solution temperature increases to the corresponding LCST of each polymer the aggregate size starts to increase. All the block copolymers exhibit clear transitions at a temperature range of 34−38 °C. Above this temperature range, large aggregates are formed with D_h values between 112 and 200 nm.

DLS technique can also be employed to investigate the pH-responsive behavior of p(NIPAM)$_{55}$-*b*-p(His)$_n$ at 37 °C by carefully adjusting the solution pH to a desired value with 5% HCl and 5% NaOH. In the solution pH range between 6.5 and 10, the aggregate size is around 150 nm (Figure 1c). Lowering of the solution pH to 5.6, a noticeable transition in the aggregate size is observed. Further lowering the solution pH, very large aggregates are observed and the aggregate size increases with the decrease of pH, irrespective of the composition of block copolymer. As the aggregates become bigger, the solutions change to visually turbid slurries. These results indicate that aggregation behavior of the block copolymer is dependent on the solution pH, most probably due to p(His) block in the copolymer. For the design of the pH responsible polymers alkaline or acidic functionality is presented to the polymer system. Unlike acidic responsive polymers that are ionized at a high pH, basic polymers are ionized at low pH conditions. p(His) is a typical example for pH-responsive and biocompatible polymer, which holds variety of applications including triggered drug release.

3.5. Self-Assembly of p(NIPAM)$_{55}$-*b*-p(His)$_n$ in Aqueous Solutions. To investigate the micelle formation by self-assembly, 10 mg of the block copolymer was dissolved in *N*,*N*-dimethyl acetamide (DMAc; 7 mL) and then deionized water (3 mL) was added slowly into the polymer solution. The resulting turbid solution was dialyzed to remove the organic solvent at 25 °C. As illustrated by transmission electron microscope (TEM) images (Figure 2), highly uniform and monodispersed spherical micelles were obtained by the self-assembly of p(NIPAM)$_{55}$-*b*-p(His)$_n$ copolymers.

The average diameter of the micelles is about 55 nm irrespective of the change of p(His) block length. As the p(His) length increases, there is an slightly increased trend losing the uniformity of micelles and forming rod−like micelles due to the aggregation of spherical micelles. Note that the spherical micelles are solid spheres as shown by scanning electron microscope (SEM) image (see inset of Figure 2a). The similar micellizations have been performed in the presence of Dox, a chemotherapeutic drug that is given to treat many different types of carcinomas, in order to determine their drug loading and release properties. The spherical shape of the micelles remains unchanged, even though the average diameter of the micelles is bigger than that of micelles fabricated in the absence of Dox by about 2-fold (see Figure 2e,f) and the size distribution of the micelles becomes somewhat broader. The drug-loading capacity of the micelles increases with increasing length of the p(His) block (Table 2), because the hydrophobic Dox drug molecules are surrounded by the p(His) block located in the core of micelles. Both inter- and intramolecular hydrophobic interactions also contribute to the improved Dox encapsulation capacity and efficiency.

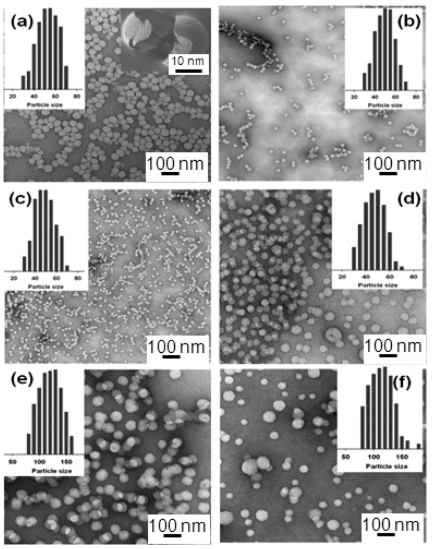

Figure 2. TEM images of the spherical micelles of p(NIPAM)-*b*-p(His) copolymers obtained by self-assembly in *N*,*N*-dimethyl acetamide/H_2O solution mixture at pH 7.4: (a) p(NIPAM)$_{55}$-*b*-(His)$_{50}$, (b) p(NIPAM)$_{55}$-*b*-p(His)$_{75}$, (c) p(NIPAM)$_{55}$-*b*-p(His)$_{100}$, and (d) p(NIPAM)$_{55}$-*b*-p(His)$_{125}$. (e, f) TEM images of spherical micelles of p(NIPAM)$_{55}$-*b*-p(His)$_{100}$ and p(NIPAM)$_{55}$-*b*-p(His)$_{125}$, respectively, self-assembled in the presence of Dox molecules. Inset of (a) is a SEM image of a broken micelle of obtained by p(NIPAM)$_{55}$-*b*-(His)$_{50}$ and the other insets in each image show size distribution.

3.6. Stimuli Responsive Release of Dox. The time-dependent release of Dox with different temperatures and pHs was evaluated by dialysis method by choosing the p(NIPAM)$_{55}$-*b*-p(His)$_{125}$ micelles (Figure 2f) as a representative sample in phosphate buffered saline (PBS, pH 7.4). Drug release experiments were evaluated by UV−vis spectrometer at 480 nm, which is the characteristic absorption maximum of Dox in solution. The release performance was observed for 60 h, and the release profiles are shown in Figure 3. The release of DOX from p(NIPAM)$_{55}$-*b*-p(His)$_{125}$ micelles was enhanced especially at 37 °C, where the percent release increased greatly, but was very slow at 15 and 25 °C, indicating that the release rate enhanced around the transition temperature of the p(NIPAM) polymer. Evidently the temperature sensitivity of the micelles is considered to be given by alteration of the polymer chain from the hydrophilic state to the hydrophobic state in response to

dx.doi.org/10.1021/bm400089m | *Biomacromolecules* XXXX, XXX, XXX−XXX

Table 2. Average Diameter and Its Distribution of $p(NIPM)_{55}$-*b*-$p(His)_n$ Micelles Fabricated by Self-Assembly before and after Dox Encapsulation, and the Resulting Drug Loading Content (DLC) and Drug Loading Efficiency (DLE)

		blank micelles		Dox-loaded micelles at 20:1 (*w*/*w*)[a]			
sample	pH	cumulant diameter	particle size distribution	cumulant diameter	particle size distribution	DLC (%)	DLE (%)
$p(NIPAM)_{55}$-*b*-$p(His)_{50}$	8.0	46.3 ± 0.1	0.11 ± 0.01	110.8 ± 2.3	0.19 ± 0.02		
	7.4	53.1 ± 0.9	0.12 ± 0.03	123.8 ± 3.1	0.32 ± 0.06		
	6.8	62.4 ± 0.2	0.37 ± 0.06	136.2 ± 1.4	0.28 ± 0.07	11.8	36.0
	6.5	74.5 ± 0.3	0.43 ± 0.07	140.1 ± 1.9	0.11 ± 0.06		
	6.0	80.1 ± 0.6	0.75 ± 0.06	160.6 ± 3.2	0.68 ± 0.05		
	5.6	90.6 ± 0.8	0.45 ± 0.02	180.6 ± 0.8	0.98 ± 0.10		
$p(NIPAM)_{55}$-*b*- $p(His)_{75}$	8.0	50.1 ± 0.6	0.18 ± 0.04	130.8 ± 1.6	0.11 ± 0.09		
	7.4	67.9 ± 1.3	0.38 ± 0.01	116.1 ± 1.2	0.19 ± 0.01		
	6.8	63.5 ± 0.9	0.12 ± 0.09	136.5 ± 3.1	0.35 ± 0.03	13.1	41.0
	6.5	68.3 ± 2.1	0.31 ± 0.07	160.2 ± 1.3	0.42 ± 0.05		
	6.0	70.1 ± 1.6	0.72 ± 0.06	140.3 ± 1.9	0.63 ± 0.01		
	5.6	96.6 ± 1.4	0.54 ± 0.02	167.6 ± 0.8	0.89 ± 0.80		
$p(NIPAM)_{55}$-*b*-$p(His)_{100}$	8.0	54.4 ± 0.6	0.71 ± 0.07	165.1 ± 2.4	0.82 ± 0.03		
	7.4	63.6 ± 1.8	0.32 ± 0.03	220.6 ± 2.4	0.31 ± 0.09		
	6.8	70.3 ± 3.5	0.48 ± 0.01	280.1 ± 1.3	0.61 ± 0.06	14.2	46.0
	6.5	68.0 ± 2.6	0.66 ± 0.08	220.0 ± 3.8	0.75 ± 0.09		
	6.0	80.1 ± 4.8	0.62 ± 0.04	268.0 ± 4.9	0.42 ± 0.02		
	5.6	100.3 ± 1.4	0.84 ± 0.02	285.6 ± 0.8	0.87 ± 0.10		
$p(NIPAM)_{55}$-*b*-$p(His)_{125}$	8.0	70.4 ± 0.9	0.61 ± 0.02	170.1 ± 2.4	0.31 ± 0.07		
	7.4	82.3 ± 0.4	0.12 ± 0.06	144.1 ± 0.7	0.42 ± 0.05		
	6.8	79.3 ± 2.9	0.63 ± 0.05	134.3 ± 1.6	0.57 ± 0.03	15.8	51.0
	6.5	68.0 ± 1.1	0.71 ± 0.62	150.4 ± 2.5	0.81 ± 0.15		
	6.0	94.1 ± 3.4	0.37 ± 0.04	257.3 ± 4.1	0.65 ± 0.61		
	5.6	110.3 ± 4.7	0.94 ± 0.02	298.6 ± 5.8	0.87 ± 0.10		

[a]Feed ratio of polymer to Dox. All measurements were performed in triplicate at 37 °C.

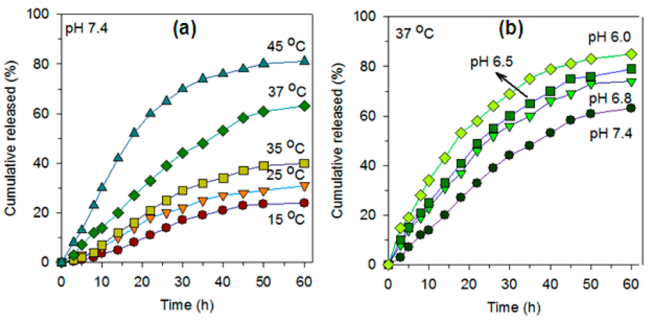

Figure 3. Time-dependent release of Dox from the $p(NIPAM)_{55}$-*b*-$p(His)_{125}$ micelles fabricated by self-assembly in phosphate-buffered saline (PBS) at pH 7.4 and different temperatures (a) at 37 °C and different pH values (b).

the ambient temperature, revealing the response at a desired temperature are obtained by the modification with p(NIPAM) polymers having LCST at that temperature.[38] The increase in hydrophobicity of the p(NIPAM) chain with raising temperature induces low solubility of the polymer in water, resulting in destabilization of the micelle. Consequently, the LCST of p(NIPAM) chains clearly affect the drug release from micelle at their transition temperature. Thus, the fixation of the p(NIPAM) chains on the micelles enhances the Dox release at the LCST of the polymer, as well as the leakage of Dox by thermally responsive micelles during the thermal transition of p(NIPAM) chain.

The influence of pH on the release rate was investigated by performing a set of time−dependent release experiments of Dox at different pH conditions with the micelles of $p(NIPAM)_{55}$-*b*-$p(His)_{125}$. Controlling the pH of the micellar solution below 7, the stable micelles start to ionize due to the imidazole side chains of p(His) block. While lowering pH of micellar solution, the imidazole rings are protonated. Protonated imidazole ring bears two N−H bonds and has a positive charge. This charge is equally distributed between both nitrogens and can be represented with two equally important resonance structures. As the degree of ionization of p(His) block of increases, the hydrophobic interactions become weakened, favoring the release of Dox. As shown in Figure 3, 62% of the incorporated Dox is released within 60 h in PBS at pH 7.4. The release rate is accelerated at acidic pH conditions, thus, the value increases to 74, 79, and 90% at pH 6.8, 6.5, and 6.0, respectively. The accelerated rate especially at pH 6.0 might be related with pK_a (~6.0) of the imidazole side chain of p(His) block. These data clearly demonstrating the release rate is sensitive to pH due to the pH-induced destabilization of the p(His) block of the micelles. Because p(His) block is an ionizable basic unit, its swelling behavior greatly depends on the pH due to the ionization−deionization of the imidazole ring on the p(His) block. Under acidic conditions, the p(His) blocks is ionized and the charged imidazole groups repel each other such that this leads to high swelling. The stability of the Dox molecules is enhanced due its ionization at the low pH environment and results in an increased diffusivity averting all nonbonding interactions with the polymer walls.

3.7. Cytotoxicity of p(NIPAM)-*b*-p(His) Micelles. Biocompatiability is a fundamental prerequisites for any in vivo biomedical applications, so the cytotoxicity and antitumor activity of the nanosized micelles of $p(NIPAM)_{55}$-*b*-$p(His)_n$ at various concentrations toward RAW264.7 mouse macrophage and HepG2 human hepatocellular carcinoma cell lines were determined by thiazolyl blue tetrazolium bromide (MTT) cell

dx.doi.org/10.1021/bm400089m | *Biomacromolecules* XXXX, XXX, XXX−XXX

proliferation assay. The absorbance of a formazan crystal at 560 nm reflects the number of living cells, because it is linearly proportional to cell numbers in a reasonable range. The cell viability percent was an average absorbance of polymer micelles at different concentrations divided by that of corresponding control sample. The cell-only group was used as control in each experiment, and the absorbance of it was similar among eight parallel experiments. Compared to control, the viability of RAW264.7 and HepG2 normal cells was higher than 80% in a wide polymer concentration range from 0.1 to 100 μg mL^{-1} (Figure 4), demonstrating all the polymer micelles have similar

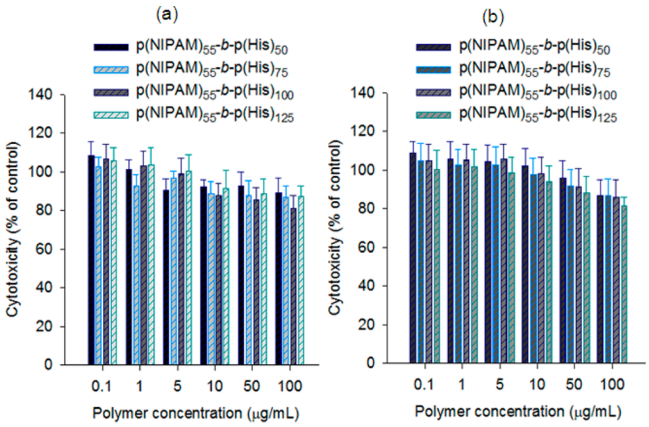

Figure 4. Cytotoxicity of the micelles of p(NIPAM)$_{55}$-*b*-p(His)$_n$ at various concentrations toward (a) RAW264.7 mouse macrophage cells and (b) HepG2 normal cells. The cell viability percent is an average absorbance of the polymer micelles group at different concentrations divided by that of corresponding control (cell only) group, the absorbance of which was similar among eight parallel experiments.

cytotoxicity against both cells regardless of the size of p(His) block. These results clearly show that the copolymer micelles fabricated by self-assembly have no acute and intrinsic cytotoxicity against normal cells.

3.8. Cellular Uptake and Cytotoxicity of Dox-Loaded p(NIPAM)-*b*-p(His) Micelles. The intracellular traffiking of the p(NIPAM)$_{55}$-*b*-p(His)$_{125}$ micelles bearing Dox in the cellular level was studied in HepG2 cells by controlling the pH of the micellar solution from pH 8 to pH 5.6 at 4, 25, and 37 °C (Figure 5). The Dox-loaded p(NIPAM)$_{55}$-*b*-p(His)$_{125}$

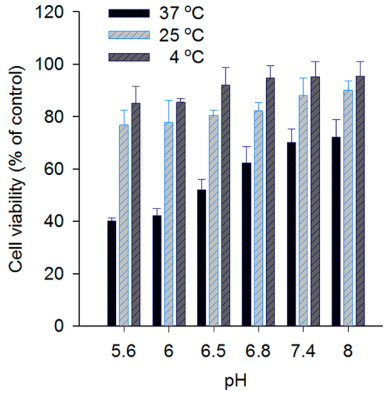

Figure 5. Anticancer activity of Dox-loaded micelles (1 μg Dox concentration) to HepG2 hepatocellular cancer (HCC) cells after 48 h incubation: p(NIPAM)$_{55}$-*b*-p(His)$_{125}$ micelles at different temperature and pH conditions.

micelles have obvious pH and temperature sensitivity and cancer cell survivability by Dox. The Dox-loaded micelles show decreased cytotoxicity at lower temperature (4 °C), and the viability of cancer cells is higher than 80% at all treatments. Due to the temperature and pH sensitivity of the Dox-loaded micelle, the cancer cell viability decreases gradually at 25 °C and sharply at 37 °C, especially under acidic pH conditions. The cell viability is about 42% at 37 °C at pH 6. The relative toxicities of free Dox and Dox-loaded nanoparticles in various cell lines were recently investigated.[39] We found that the in vitro half-maximal inhibitory concentration (IC_{50}) values for free Dox and Dox-loaded p(NIPAM)$_{55}$-*b*-p(His)$_{125}$ micelles on HepG2 cells were 0.061 ± 0.002 and 0.115 ± 0.005 μM, respectively, at pH 7.4 after 24 h incubation.

The cells were then observed by the confocal laser scanning microscope (CLSM) in order to get further clarification on the pH- and temperature-dependent endocytosis of the Dox-loaded micelles and the results are illustrated in Figure 6. The Dox-loaded p(NIPAM)$_{55}$-*b*-p(His)$_{125}$ micelles efficiently deliver and release Dox molecules into the cell nucleus. As expected, stronger fluorescence is clearly observed at acidic conditions and at 37 °C. At 4 °C, fluorescence of cells was not significantly changed as shown in Figure 6a, indicating that the endocytosis mechanism of cells became idle at low temperature and then the uptake of nanoparticles might be minimized regardless of pH changes. For further confirmation, Dox accumulated HepG2 cells were analyzed using flow cytometer (Figure S7 in SI). The fluorescence intensity of the Dox-loaded micelles is greatly enhanced at acidic conditions near body temperature. Considering the extracellular pH of cancer tissue is acidic (around pH 6.8), pH-sensitive polymeric micelles, specifically at acidic pH have advantages to release the drug into cancer cells. Because the pH of normal tissue and bloodstream is about 7.4, Dox-loaded micelles can selectively kill the cancer cells due to the pH-induced destabilization of the micelle and subsequent delivery of the anticancer drug at pH 6.0−6.8 at around body temperature.[40] Fluorescence analysis of cancer cells revealed that Dox-loaded micelles showed increased fluorescence intensity at acidic pH, indicating that the Dox-loaded p(NIPAM)$_{55}$-*b*-p(His)$_n$ micelles have tumor-extracellular pH-sensitive targetability. Furthermore, Dox-loaded p(NIPAM)$_{55}$-*b*-p(His)$_{125}$ micelles have a capability for temperature-sensitive endocytosis for HepG2 tumor cells.

4. CONCLUSION

We have developed a series of novel biocompatible p(NIPAM)$_{55}$-*b*-p(His)$_n$ (n = 55, 75, 100, 125) chimeric polymers have been successfully synthesized by combining RAFT polymerization with the p(NIPAM) macroinitiated ROP of His−NCA and evaluated them as stimuli-responsive drug carrier for tumor targeting. Dox can be efficiently loaded in the self-assembled spherical micelles of p(NIPAM)-*b*-p(His) in nanoscale that are stable under extracellular conditions but are destabilized under acidic environments where tumor cells are located. The highly uniform micelles show excellent Dox-loading efficiency and the Dox-loaded micelles show pH- and temperature-dependent delivery of internalized Dox to the HepG2 human hepatocellular cancer cells. The enhanced anticancer activity at 37 °C specifically under acidic environments adds the value of the p(NIPAM)-*b*-p(His) chimeric polymers as new dual-sensitive tumor targeting drug delivery materials.

dx.doi.org/10.1021/bm400089m | *Biomacromolecules* XXXX, XXX, XXX−XXX

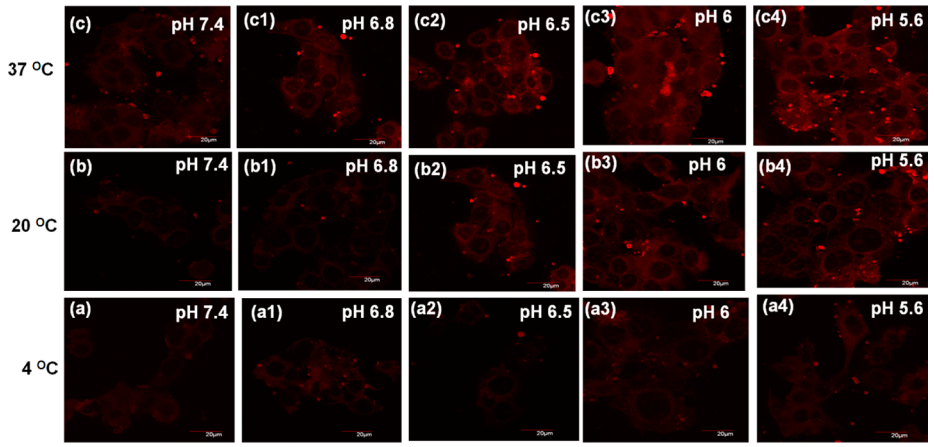

Figure 6. CLSM images of HepG2 hepatocellular cancer cells after 3 h incubation taken at different pH and temperature conditions with Dox-loaded p(NIPAM)$_{55}$-*b*-p(His)$_{125}$ micelles at 4 °C (a–a4), 20 °C (b–b4), and at 37 °C (c–c4). Scale bar = 20 μm.

■ ASSOCIATED CONTENT

Supporting Information

Synthesis procedure of CTA-1, characterization of block copolypeptides and their intermediates, and flow cytometric analysis of HepG2 hepatocellular carcinoma cells after the internalization of Dox-loaded micelles are available. This material is available free of charge via the Internet at http://pubs.acs.org.

■ AUTHOR INFORMATION

Corresponding Author

*E-mail: ilkim@pusan.ac.kr.

Notes

The authors declare no competing financial interest.

■ ACKNOWLEDGMENTS

This work was supported by grants-in-aid for the World Class University Program (No. R32–2008–000–10174–0), the Fusion Research Program for Green Technologies through the National Research Foundation of Korea from MEST (No. 2012M3C1A1054502), and Korea Healthcare Technology R&D Project from the Ministry for Health Welfare and Family Affairs (A091047).

■ REFERENCES

(1) Osada, Y.; Gong, J. P. *Adv. Mater.* **1998**, *10*, 827–837.
(2) Lee, E. S.; Na, K.; Bae, Y. H. *Nano Lett.* **2005**, *5*, 325–329.
(3) Mart, R. J.; Osborne, R. D.; Stevens, M. M.; Ulijn, S. V. *Soft Matter* **2006**, *10*, 822–835.
(4) McCormick, C. L.; Sumerlin, B. S.; Lokitz, B. S.; Stempka, J. E. *Soft Matter* **2008**, *9*, 1760–1773.
(5) Schmaljohann, D. *Adv. Drug Delivery Rev.* **2006**, *58*, 1655–1670.
(6) Zhang, J.; Pelton, R.; Deng, Y. *Langmuir* **1995**, *11*, 2301–2302.
(7) Maeda, Y.; Yamamoto, H.; Ikeda, I. *Langmuir* **2001**, *17*, 6855–6859.
(8) Yin, X.; Hoffman, A. S.; Stayton, P. S. *Biomacromolecules* **2006**, *7*, 1381–1385.
(9) Bisht, H. S.; Wan, L.; Mao, G.; Oupicky, D. *Polymer* **2005**, *46*, 7945–7952.
(10) Zhu, P. W.; Napper, D. H. *Macromolecules* **1999**, *32*, 2068–2070.
(11) Convertine, A. J.; Lokitz, B. S.; Vasileva, Y.; Myrick, L. J.; Scales, C. W.; Lowe, A. B.; McCormick, C. L. *Macromolecules* **2006**, *39*, 1724–1730.
(12) Qin, S.; Geng, Y.; Discher, D. E.; Yang, S. *Adv. Mater.* **2006**, *18*, 2905–2909.
(13) Mei, A.; Guo, X.; Ding, Y.; Zhang, X.; Xu, J.; Fan, Z.; Du, B. *Macromolecules* **2010**, *43*, 7312–7320.
(14) Kohori, F.; Sakai, K.; Aoyagi, T.; Yokoyama, M.; Sakurai, Y.; Okano, T. *J. Controlled Release* **1998**, *55*, 87–98.
(15) Nakayama, M.; Okano, T.; Miyazaki, T.; Kohori, F.; Sakai, K.; Yokoyama, M. *J. Controlled Release* **2006**, *115*, 46–56.
(16) Nakayama, M.; Okano, T. *Macromolecules* **2008**, *41*, 504–507.
(17) Cheng, J. H.; Feng, C. C. *Macromolecules* **2008**, *41*, 7041–7052.
(18) Hawker, C. J.; Bosman, A. W.; Harth, E. *Chem. Rev.* **2001**, *101*, 3661–3688.
(19) Matyjaszewski, K.; Xia, J. *Chem. Rev.* **2001**, *101*, 2921–2990.
(20) Moad, G.; Rizzardo, E.; Thang, S. H. *Aust. J. Chem.* **2006**, *59*, 669–692.
(21) Barner, L.; Davis, T. P.; Stenzel, M. H.; Barner-Kowollik, C. *Macromol. Rapid Commun.* **2007**, *28*, 539–559.
(22) Boyer, C.; Bulmus, V.; Davis, T. P.; Ladmiral, V.; Liu, J.; Perrier, S. *Chem. Rev.* **2009**, *109*, 5402–5436.
(23) Borner, H. G. *Macromol. Chem. Phys.* **2007**, *208*, 124–130.
(24) Klok, H. A. *Macromolecules* **2009**, *42*, 7990–8000.
(25) Rao, J.; Luo, Z.; Ge, Z.; Liu, H.; Liu, S. *Biomacromolecules* **2007**, *8*, 3871–3878.
(26) Xiuqiang, Z.; Jingguo, L.; Wen, L.; Afang, Z. *Biomacromolecules* **2007**, *8*, 3557–3567.
(27) Lin, D.; Keyu, S.; Yuying, Z.; Haimei, W.; Jianguo, Z.; Xianzhi, G.; Zongjie, D.; Baolong, Z. *J. Colloids Interface Sci.* **2008**, *323*, 169–175.
(28) Zhang, X.; Monge, S.; In, M.; Giani, O.; Robin, J.-J. *Soft Matter* **2013**, *9*, 1301–1309.
(29) Pichon, C.; Goncalves, C.; Midoux, P. *Adv. Drug Delivery Rev.* **2001**, *53*, 75–94.
(30) Carlsen, A.; Lecommandoux, S. *Curr. Opin. Colloid Interface Sci.* **2009**, *14*, 329–339.
(31) Sanson, C.; Schatz, C.; Meins, J-F. L.; Soum, A.; Thevenot, J.; Garanger, E.; Lecommandoux, S. *J. Controlled Release* **2010**, *147*, 428–435.
(32) Upadhyay, K. K.; Meins, J-F. L.; Misra, A.; Voisin, P.; Bouchaud, V.; Ibarboure, E.; Schatz, C.; Lecommandoux, S. *Biomacromolecules* **2009**, *10*, 2802–2808.
(33) Johnson, R P.; Jeong, Y. I.; Chung, C. W.; Kang, D. H.; Oh, S. O.; Suh, H.; Kim, I. *Adv. Funct. Mater.* **2012**, *22*, 1058–1068.
(34) Boyer, C.; Stenzel, M. H.; Davis, T. P. *J. Polym. Sci., Part A: Polym. Chem.* **2011**, *49*, 551–595.
(35) Zhang, X.; Oddon, M.; Giani, O.; Monge, S.; Robin, J.-J. *Macromolecules* **2010**, *43*, 2654–2656.
(36) Ganachaud, F.; Monteiro, M. J.; Gilbert, R. G.; Dourges, M. A.; Thang, S. H.; Rizzardo, E. *Macromolecules* **2000**, *33*, 6738–6745.

(37) Eun, S. G.; Samuel, M. H. *Prog. Polym. Sci.* **2004**, *29*, 1173−1222.
(38) Hayashi, H.; Kono, K.; Takagishi, T. *Bioconjugate Chem.* **1999**, *10*, 412−418.
(39) Duong, H. T. T.; Hughes, F.; Sagnella, S.; Kavallaris, M.; Macmillan, A.; Whan, R.; Hook, J.; Davis, T. P.; Boyer, C. *Mol. Pharmaceutics* **2012**, *9*, 3046−3061.
(40) Lee, E. S.; Shin, H. J.; Na, K.; Bae, Y. H. *J. Controlled Release* **2003**, *90*, 363−374.